

Scientific Excellence • Resource Protection & Conservation • Benefits for Canadians
Excellence scientifique • Protection et conservation des ressources • Bénéfices aux Canadiens

SAR SENSITIVITIES TO SURFACE GRAVITY WAVES

J.R. Keeley

Marine Environmental Data Services Branch
Department of Fisheries and Oceans
Ottawa, Ontario, K1A 0E6

1992

**Canadian Technical Report of
Hydrography and Ocean Sciences 105**



Fisheries
and Oceans

Pêches
et Océans

Canada

Canadian Technical Report of Hydrography and Ocean Sciences

Technical reports contain scientific and technical information that contributes to existing knowledge but which is not normally appropriate for primary literature. The subject matter is related generally to programs and interests of the Ocean Science and Surveys (OSS) sector of the Department of Fisheries and Oceans.

Technical reports may be cited as full publications. The correct citation appears above the abstract of each report. Each report is abstracted in *Aquatic Sciences and Fisheries Abstracts* and indexed in the Department's annual index to scientific and technical publications.

Technical reports are produced regionally but are numbered nationally. Requests for individual reports will be filled by the issuing establishment listed on the front cover and title page. Out of stock reports will be supplied for a fee by commercial agents.

Regional and headquarters establishments of Ocean Science and Surveys ceased publication of their various report series as of December 1981. A complete listing of these publications is published in the *Canadian Journal of Fisheries and Aquatic Sciences*, Volume 39: Index to Publications 1982. The current series, which begins with report number 1, was initiated in January 1982.

Rapport technique canadien sur l'hydrographie et les sciences océaniques

Les rapports techniques contiennent des renseignements scientifiques et techniques qui constituent une contribution aux connaissances actuelles, mais qui ne sont pas normalement appropriés pour la publication dans un journal scientifique. Le sujet est généralement lié aux programmes et intérêts du service des Sciences et levés océaniques (SLO) du ministère des Pêches et des Océans.

Les rapports techniques peuvent être cités comme des publications complètes. Le titre exact paraît au-dessus du résumé de chaque rapport. Les rapports techniques sont résumés dans la revue *Résumés des sciences aquatiques et halieutiques*, et ils sont classés dans l'index annuel des publications scientifiques et techniques du Ministère.

Les rapports techniques sont produits à l'échelon régional, mais numérotés à l'échelon national. Les demandes de rapports seront satisfaites par l'établissement auteur dont le nom figure sur la couverture et la page du titre. Les rapports épuisés seront fournis contre rétribution par des agents commerciaux.

Les établissements des Sciences et levés océaniques dans les régions et à l'administration centrale ont cessé de publier leurs diverses séries de rapports en décembre 1981. Une liste complète de ces publications figure dans le volume 39, Index des publications 1982 du *Journal canadien des sciences halieutiques et aquatiques*. La série actuelle a commencé avec la publication du rapport numéro 1 en janvier 1982.

**Canadian Technical Report of
Hydrography and Ocean Sciences 105**

1992

**SAR SENSITIVITIES
TO SURFACE GRAVITY WAVES**

by

J. R. Keeley

**Marine Environmental Data Service
Department of Fisheries and Oceans**

Ottawa, Ontario

K1A 0E6

© Minister of Supply and Services Canada 1992
Cat. No. Fs97-18/105E ISSN 0711-6764

Correct citation for this publication:

Keeley, J.R. 1992. SAR sensitivities to surface gravity waves.
Can. Tech. Rep. Hydrogr. Ocean Sci. 105: 21 p.

Contents

	Page
Abstract	v
Résumé	v
Introduction	1
The Data Collection	1
Preliminary Data Analyses	2
Antenna Wobble	4
Incidence Angle Dependence	6
SAR Look Direction and Wave Orientation	8
Wind Speed and Wave Height Dependence	14
Conclusion	14
Acknowledgements	14
References	15

Abstract

Keeley, J.R. 1992. SAR sensitivities to surface gravity waves. Can. Tech. Rep. Hydrogr. Ocean Sci. 105: 21 p.

In March of 1982, two experiments using a synthetic aperture radar, SAR, were conducted over a drilling platform near Sable Island, Nova Scotia. The object of the experiment was to learn something about the sensitivities of the SAR to detecting surface gravity waves from a variety of radar orientations and in different wave conditions. The experiments occurred over two separate days with differing wave conditions. Results are presented for the sensitivity of the radar to antenna wobble, changing incidence angle, and the detection of the same waves at differing radar orientations.

Résumé

Keeley, J.R. 1992. SAR sensitivities to surface gravity waves. Can. Tech. Rep. Hydrogr. Ocean Sci. 105: 21 p.

En mars 1982, un radar à antenne synthétique (SAR) a fait l'objet de deux expériences sur une plate-forme de forage mouillée près de l'île de Sable (Nouvelle-Écosse). Ces expériences visaient la collecte de données sur la sensibilité du SAR pour la détection d'ondes de gravité de surface dans différentes positions et pour divers régimes d'ondes. Les expériences ont été effectuées au cours de deux jours où les régimes d'ondes ont varié. Les résultats présentés portent sur la sensibilité du radar en fonction du tremblement de l'antenne, sur la variation de l'angle d'incidence et sur la détection des mêmes ondes à diverses positions du radar.

Introduction

The Canadian government has a program directed to the goal of operating a satellite with a synthetic aperture radar (SAR) on board. This satellite has been named RADARSAT and is scheduled for operation sometime in the early 1990s. It will be placed in an orbit which will carry it over the Canadian Arctic. One of its main goals is to monitor ship traffic and ice conditions. For this purpose a SAR performs well since it can operate in day or night, can resolve ships from orbit, and can receive signals from the ocean surface in all weather conditions.

A SAR has shown value in other studies as well (Lapp and Lapp 1981; Beal, DeLeonibus and Katz 1981). To broaden the use of the SAR, a number of study teams have been organized to investigate the applications such a satellite might have to Canada. The Oceans Team has been concerned with investigating the utility of SAR data in studying oceanic processes. In support of this, the Canada Centre for Remote Sensing (CCRS) has made available for experiments, its Convair 580 aircraft and the SAR which is mounted on board.

A number of studies have been conducted to examine the visibility of surface gravity waves to a SAR. Many of these made use of data from SEASAT (Gonzales et al. 1979; Fu and Holt 1982). A partial review of relevant papers is given by Brown and Cheney (1983). These analyses often did not have surface data collections to which comparisons could be made because the satellite had such a short operating lifetime. As a consequence, the results have shown, only partially, some of the capabilities of a SAR. Two of the factors which receive further attention here are the dependence of wave visibility on the radar beam incidence angle and the relative look angle between the radar and the wave field. These have been addressed both theoretically or experimentally by Raney (1981); Alpers, Ross and Rufenach (1981) and Shuchman et al. (1983), among others, but not with the range of variation which this experiment provided.

In March of 1982, the Convair flew two missions over the drilling platform, the Rowan Juneau, operated by Mobil Oil of Canada, positioned near Sable Island. In both cases, a box was flown with the radar pointing in towards the drilling platform at the centre. Both X and C band data were collected. The results of the analyses of the data collected on these days are presented here.

The Data Collection

On March 15 and 17, SAR data were collected along flight lines flown in the pattern of an eight sided box. The aircraft flew at 3050 m with a ground speed of between 120 and 125 m/sec on March 15 and between 122 and 135 m/sec on March 17. The SAR was operated with VV polarization at both X and C band. One look, digital data were logged on magnetic tape for subsequent processing. At the same time, a real-time processor, RTP, presented the imagery to the flight crew so that adjustments could be made if necessary. Although both C and X band data were collected, only the X band data were of sufficient quality to permit further analysis. The SAR was oriented so that the near edge of the beam pointed vertically down. The range of incidence angles from near to far range was 0 to 63 degrees. With geometric corrections applied, the ground resolution was 1.42 x 1.42 meters. All eight lines were flown in the period of about 2 hours.

The rig operators cooperated in the experiment by recording 5 minute averages of the wind speed and direction during the experiment and these were made available for analysis. On March 15 the winds were blowing from about 278 degrees True and at a speed of about 18 m/sec. On March 17, the wind was from 299 degrees True at a speed of about 6 m/sec. A waverider buoy also was operating in the neighbourhood of the rig. This instrument records 20 minute sequences, with a 0.5 sec sampling interval, of the surface elevation every 3 hours. The data are recorded on magnetic tape, and forwarded to the Marine Environmental Data Service for subsequent processing to

non-directional wave height spectra. The significant wave heights and peak periods were 4.6 m and 9.9 sec for March 15 and 2.2 m and 7.9 sec for March 17.

Preliminary Data Analyses

It was thought prudent to attempt to confirm the recorded aircraft headings for each of the lines. With the flight conducted so near to Sable Island, both the rig and either the island itself or the sand banks near the island were visible in each of the RTP imagery from March 15. By using these indicators it was relatively easy to overlay the flight lines and to check the direction recorded in the logs. Table 1 presents the results of the comparisons. Variations between the overlay and the recorded direction are up to 4 degrees. Variations between these and the directions derived from the latitudes and longitudes of the start and end points of the lines are as large as 20 degrees. Since the start and end locations are recorded to only tenths of minutes there is some room for variation allowed. The directions derived from overlaying the RTPs are used as the true directions of the flight lines. For March 17, it was not possible to use features in the RTPs to determine overlaps and therefore, to check flight directions. However, given the agreement found between the two methods on March 15, the recorded directions on the 17th. are likely very close to what was actually flown.

Table 1. Flight directions derived from aircraft logs, LOG, overlaying RTPs, RTP, and calculating start and end points, S/E. Entries are given in degrees True.

<u>LINE/PASS</u>	MARCH 15			MARCH 17	
	<u>LOG</u>	<u>RTP</u>	<u>S/E</u>	<u>LINE/PASS</u>	<u>LOG</u>
2/3	189	192	172	1/1	100
3/4	280	277	276	2/2	190
4/5	10	12	14	4/4	10
5/6	145	146	136	5/5	145
6/10	234	230	246	6/6	235
				7/7	325
				8/8	55

The real-time processor imagery was used to decide how much of the data collected was to be geometrically corrected and transcribed to computer compatible form. The choice of the portions of the data to undergo further analysis was subjective. For the imagery from March 15, it was based on the visibility of waves in the image, the overlaps of one scene to another, and the uniformity of the bathymetry in the area covered. The latter was assessed from field sheets of the area prepared by the Canadian Hydrographic Service from surveys conducted in 1982. For March 17, the imagery was chosen to provide the maximum overlap between all possible scenes and, thus, to get as many coincident views of the same wave field over the same bathymetry. The transcriptions and necessary geometric corrections were made by the CCRS. The various chosen subscenes are shown in Figure 1. The small, trapezoidal shaped area east of the tip of the island, is the common overlap region for imagery from March 17. The other rectangles are the locations of the scenes derived from imagery from March 15.

The digital analyses were conducted on an image analysis system operated at the RADARSAT office in Ottawa. The analyses to be presented are based upon the Fourier analysis of various subscenes from the imagery. The data of each image consisted of 4275 pixels (this is in the range direction which is orthogonal to the flight path) by 3595 lines (in azimuth direction which is along the flight path). With the ground resolution of 1.42 m, each

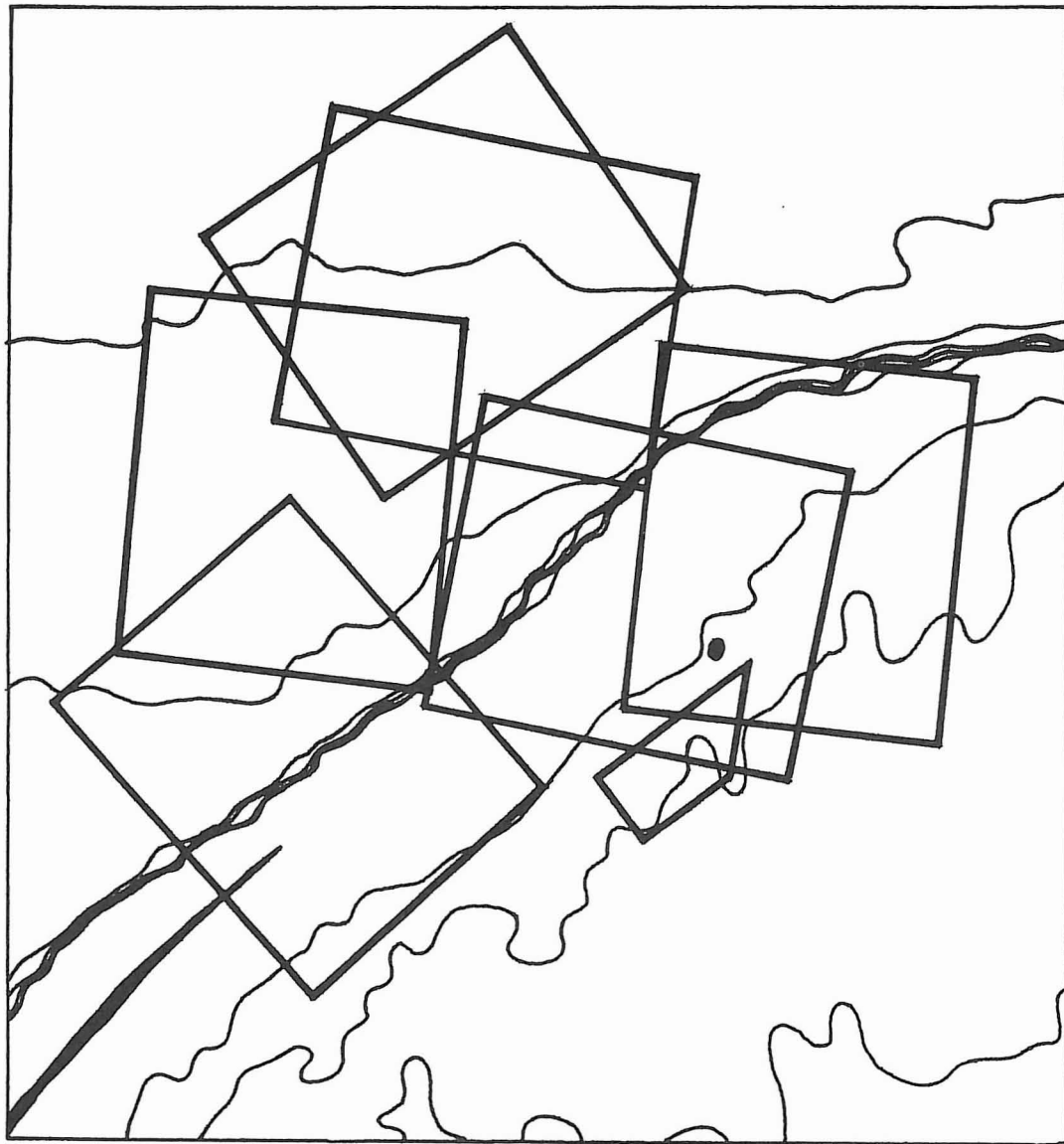


Figure 1. Map of the Sable Island area showing the location of the Rowan Juneau and the flight lines along which the SAR data were collected.

scene measured 6.04 x 5.08 km. From each image a number of subscenes were selected. A subscene was 542 x 542 pixels (766 x 766 m). This size was chosen to tradeoff the requirements of a large enough area to adequately resolve surface gravity waves and small enough that processing time was kept at a reasonable level. The image intensity was squared to derive the power of the radar return. The data were passed through a two dimensional analog of a Cartwright filter (Keeley 1982) with a cutoff at 4.96 m; that is, wavelengths shorter than the cutoff were suppressed. The resulting image was decimated by a factor of 2 to leave a subscene 256 x 256 pixels. A least squares fitted plane was subtracted from the subscene to remove any trend. Such a trend could result from variations in radar illumination of the ocean surface.

Next the subscene was normalized by the variance of the subscene. This was done to remove any effects of power variations due to differing radar illumination from one subscene to another. The subscene was next put through a fast Fourier transform. The results were squared to get a spectral density of radar intensity by wavenumber. Because of the 180 degree ambiguity in SAR data, only one half of the transform is considered although both halves are preserved. The transform was then folded up into one dimension, and examined to find the background noise level. This was specified as the average spectral density in a region of the transform where the one dimensional spectrum flattens out. Typically, this was in the range of wavelengths of about 14 m. The transform was divided by the noise estimate. To emphasize features in the transform, each was divided by the largest spectral density. A 5 x 5 Gaussian shaped filter was then passed over the image to smooth the results. The transform was then scanned automatically to locate the wavelength and orientation of the largest 40 peaks, where a peak is a local maximum in the spectral density surface, as a function of wavenumber and angle.

In each transform there are 18 degrees of freedom. Using the chi square distribution, 95 percent confidence intervals were calculated for each peak. Hand contouring of the transform, at the lower confidence interval of each peak, showed which peaks were separable, at this level of confidence, from the others.

The orientation of the waves corresponding to each significant peak was determined from the direction of the line from which the subscene was extracted and the position of the peak within the transform. In this fashion, the orientation of the waves with respect to true north was determined. In order to be able to compare the strength of the spectral density between subscenes it was necessary to reapply corrections on the scaled transform. Thus the power of each peak was divided by the scale factor and multiplied by the noise factor. The resulting estimates of the spectral density were then available for direct comparison across transforms of data collected on the same day.

Antenna Wobble

One of the images, line 2 of March 15 and shown in Figure 2, showed a banding in the visibility of the waves. While banding was visible on nearly all strips of the RTP, the processed scene from line 2 was the only one in which it appeared. The linearity of the banding from near to far range, suggested this was the result of motion of the antenna. This is borne out by the fact that the line on which this occurred was flown nearly across the wind. With strong and gusty winds, the flight crew might have had some difficulty maintaining the aircraft heading and, therefore, the antenna rigidly pointed in a fixed attitude to the ground. The analysis of this was necessary since such noticeable variations in visibility would cause substantial variations in spectral densities returned from inside (called rough regions) or outside (called smooth regions) of the bands.

The orientation of the dominant waves was nearly range travelling in the image from line 2. It is known that range travelling waves are more visible than waves at some other orientation with respect to the radar (Vesecky, Assal and Stewart 1981). Because of this, it was assumed that the "true" visibility of the wave field was represented in the rough regions. It was then necessary to quantify the difference in spectral density from rough to smooth regions so that corrections could be applied. This was done by choosing 6 subscenes over varying ranges

CANADA CENTRE FOR REMOTE SENSING

SABLE ISLAND. TR-131. 81/66

RADARSAT-SDA0137

SAR580 HRNS-X VV FLIGHT 002003 19820315161100000

FRM.CNTR.44: 1:59 N 59:35: 0 W

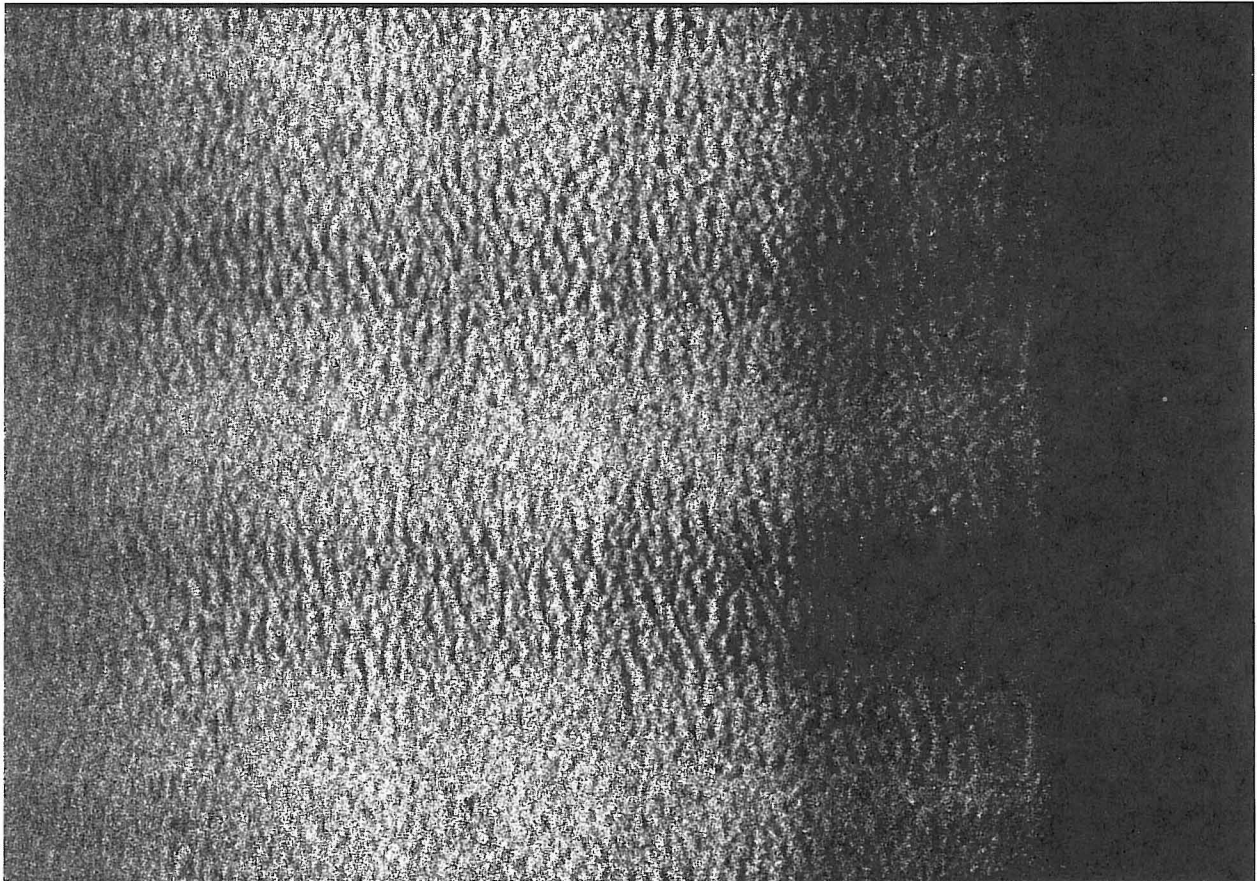
PROCESS CANADA CRC IRSPF 19821013

IMAGED 13:58 23-FEB-83

RESOLUTION: 1.4M RA X 1.4M AZ. LOOKS: 1 X 1

SCALE 0 |-----| 1.4KM

GROUND RANGE



A
Z
I
M
U
T
H

Figure 2. Radar image showing banding which was analysed for determining antenna wobble.

within the rough and smooth bands of the image. While there are known to be variations caused by the incidence angle of the radar (Alpers, Ross and Rufenach 1981), these were removed by averaging over the subscenes from near to far range. There were 2 rough and 2 smooth bands. The transforms were generated for each of the 6 subscenes within a band and then averaged. Noise estimates and scaling factors were calculated as described previously, then applied to enhance the peaks in each average. Figure 3 shows average spectra, displayed on a common scale, from the rough and smooth bands of this image. There are evident differences in strength of the major peak. Common peaks were sought by looking for the maximum values in the spectral densities at roughly the same orientation. While Figure 2 suggests crossing waves were present, only the strongest peak was used to examine the effects of antenna wobble. The spectral densities of the largest common peak are compared in Table 2.

Table 2. Comparisons of the spectral densities of image intensity and orientations of the wave crests in rough (R) and smooth (S) regions of imagery from line 2. Angles are in degrees from true north and wavelengths are in meters.

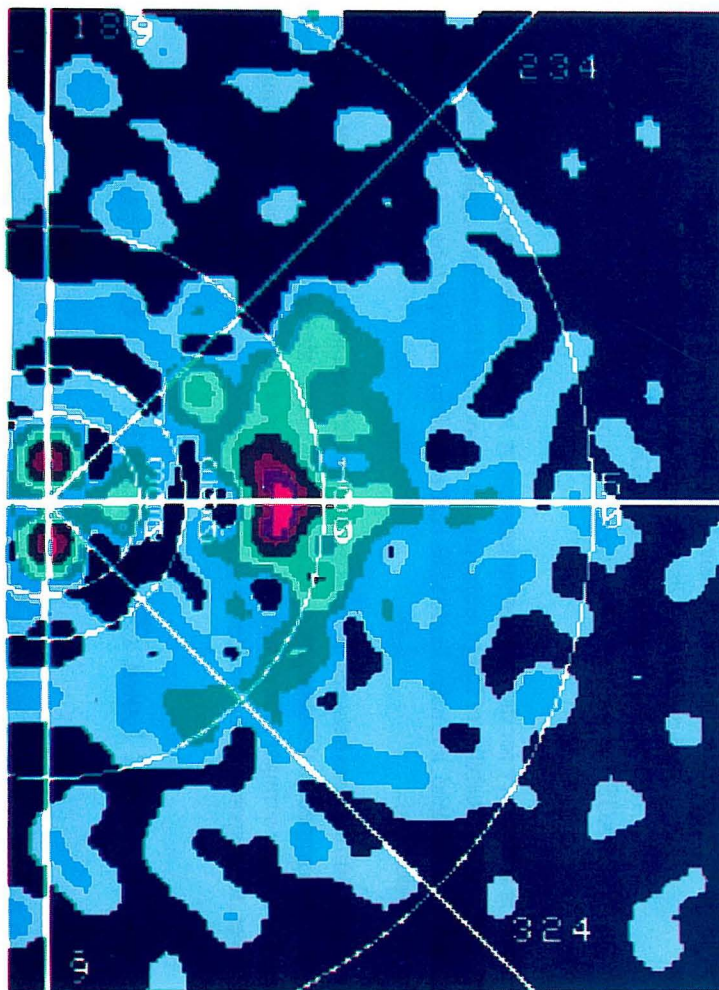
<u>BAND</u>	<u>SPECTRAL DENSITY</u>	<u>TRUE ANGLE</u>	<u>WAVE LENGTH</u>
R1	2.34	100	118
R2	3.77	81	116
S1	0.50	94	115
S2	0.80	110	110

As is evident, there is substantial variation in both spectral densities and orientation even comparing results from the two rough or smooth bands. There are visible variations between one rough band and the other, so it is not surprising that these are reflected in the spectral densities. Overall, the ratio of energy in the rough to smooth band for a common peak is about 4.7 to 1.

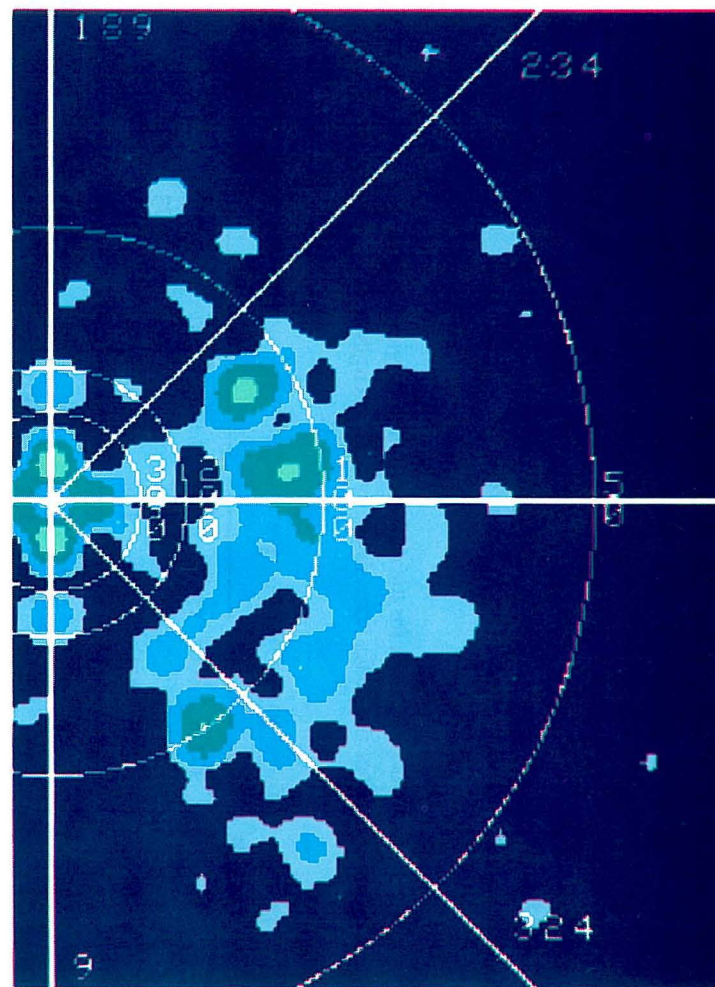
In analyses presented later, it was necessary to use subscenes located outside of the rough bands in this image. The spectral densities from these regions are multiplied by the factor 4.7 before comparisons are made to other spectra.

Incidence Angle Dependence

The strength of the radar backscatter from the ocean surface is known to be a function of the incidence angle (Alpers et al. 1981). Of more direct application for oceanographers, is a measure of the relative strengths of the same wave component when viewed at varying incidence angles. The comparison of strength of the return as a function of incidence angle is simplest and most reliable if only the strongest wave components are examined. To ensure identification from one subscene to another at varying incidence angles, a constant wave orientation is desirable. This means it is best to choose a subscene in which the bathymetry is unchanging. While the size of a subscene is less than a kilometer it is still desirable to choose an image where the depths of water are constant. Three images met this criterion; those from lines 2, 3b, and 5 (of March 15). All of these are from the north side of Sable Island and all have water depths of about 55 to 60 meters over the entire image. In these scenes, the radar had look directions which are roughly 0, 90 and 45 degrees, respectively, to the orientation of the major component of the wave field. The results can be averaged regardless of wave orientation or examined to see if wave orientation has some role in influencing the incidence angle dependence.



ROUGH



SMOOTH

Figure 3. Averaged spectra from a rough and a smooth region of line 2.

There are about 4200 pixels in the range direction. Requiring 542 x 542 for each Fourier analysis, means there are 7 subscenes available at different incidence angles and which are independent. Because there are about 3600 pixels in azimuth, there are 6 subscenes available for each incidence angle. The analysis divided each of the images into 6 by 7 subscenes. Fourier transforms were calculated as described earlier. There were a number of peaks which showed up in the individual spectra and proved to show a consistency in orientation and wavelength across the subscene. It was decided that if more peaks could be used, and these at different orientations with respect to the radar, a more stable estimate of the incidence angle dependence could be gained. In the end, the two wave components with the strongest return were used to calculate the incidence angle dependence. The results are displayed in Table 3. Figure 4 shows averaged spectra from incidence angles of 10, 30, and 80 degrees (labeled near, mid, and far range) and gives a visual presentation of some of the information of Table 3. Gaps in the table result when one of the components could not be identified.

Table 3. Incidence angle dependences for the different lines. Angles are in degrees and table entries are the relative strength of the peaks normalized by peak strength at 11°.

LINE: ANGLE	2		5		3b		AVERAGE
11	1.000	1.000	1.000	1.000	1.000	1.000	1.000
23	.343		1.116	.859	.559	.989	.773
35	.118	.031	.148	.116	.145	.233	.132
43	.037	.041	.080	.022	.138	.147	.078
51	.054		.076	.024	.131	.126	.082
57	.114		.104	.101	.375	.173	.173
61	.218		.197	.103	.365	.368	.250

2 = results from line 2 (SDA-137, 0 degrees)

3b = results from line 3b (SDA-132, 90 degrees)

5 = results from line 5 (SDA-129, 45 degrees)

AVERAGE = average normalized power over all look directions.

There is a tendency for the response to increase at higher incidence angles. Although for large angles there is the theoretical possibility of Bragg scattering at a harmonic of the surface capillary wave wavelength this is not likely the cause. Instead, it is more likely to be contamination from sidelobes of the radar beam. (R.K Raney, personal communication).

There are differences between the responses at the different look angles. Those at 45 and 90 degrees (and these are only with respect to the strongest wave component) show similar behaviour at low incidence angles. At higher angles, there are stronger returns with the main component oriented as azimuth travelling waves. For range oriented waves, the response at low incidence angles is lower than at other orientations to the radar beam.

SAR Look Direction and Wave Orientation

From previous studies it is known that the visibility of surface waves is dependent upon the radar look direction with respect to the wave orientation (Shuchman et al. 1983). A quantitative study of this dependence using SEASAT data is not possible, since the satellite did not last long enough to provide data from a variety of

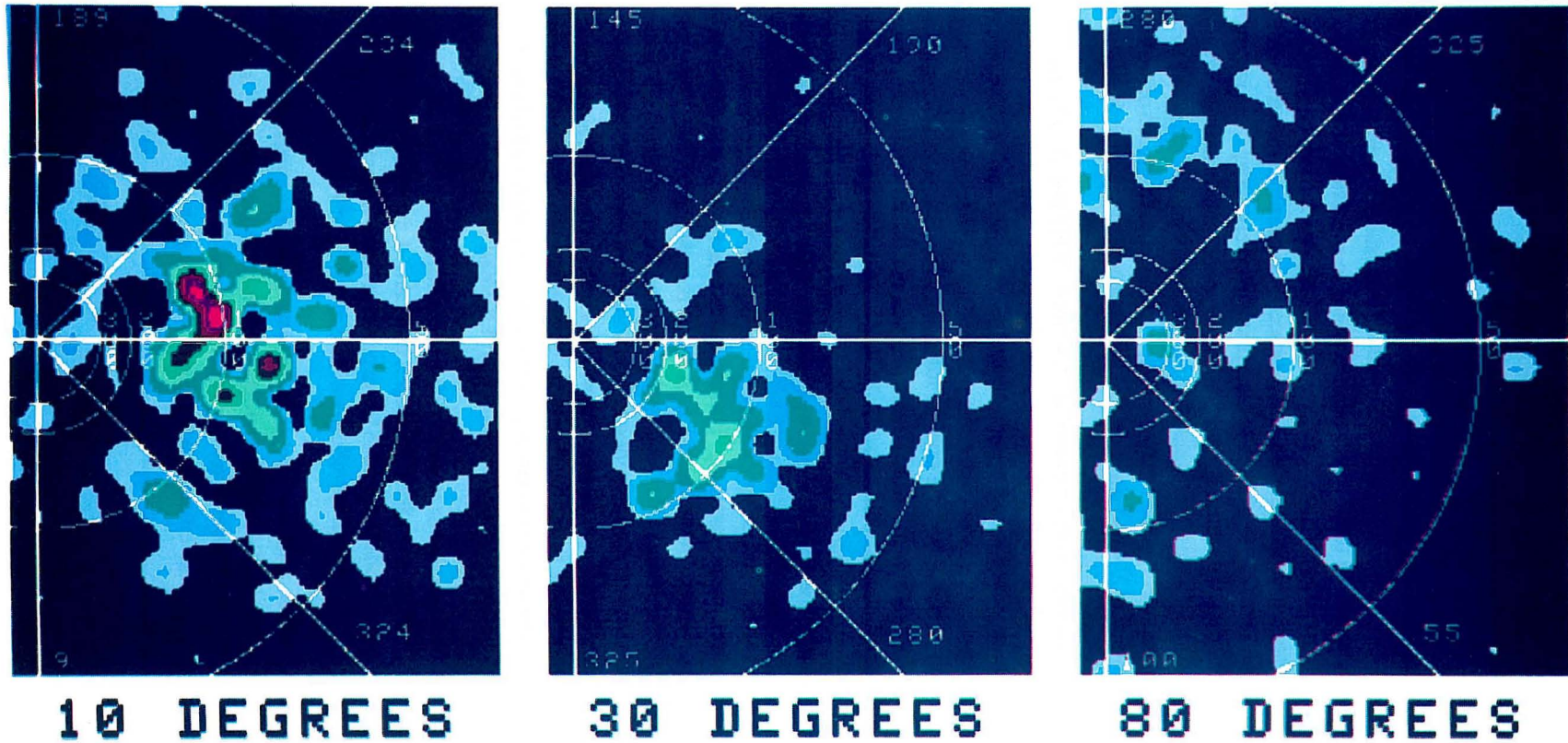


Figure 4. Averaged spectra from incidence angles of 10, 30 and 80 degrees from line 5.

wave directions from areas where wave buoys existed. Since then, a number of studies have looked at this dependence but not with the same degree of directional resolution as provided by the Sable Island data nor from an analysis of digitally recorded SAR data. The latter is desirable, since many powerful computer processing techniques may be applied to the analysis.

If the data had been collected over a region where the waves were propagating largely undisturbed by bathymetry, that is in deep water, the determination of the radar look direction to wave orientation dependence would have been simplified. However, the area around Sable Island has marked depth variations so that wave refraction cannot be ignored. In order to negate effects due to refraction, it was necessary to find overlapping subscenes from the various images from the different lines. This was done by constructing overlays of each image with respect to the drilling rig and choosing as many subscenes as possible from the overlapping regions. Because these are from varying orientations to true north, exact pixel for pixel overlaps, are impossible. However, overlaps about the subscene centres were obtained. All possible overlaps were examined from the digital images which were available. From March 15, this constituted 28 overlaps mostly in pairs but with 5 subscenes overlapping for a triplet of images. From March 17, there were 7 overlapping subscenes from each of the 9 scenes examined. Again, results were only examined at X-band since the C-band data proved of unsuitable quality.

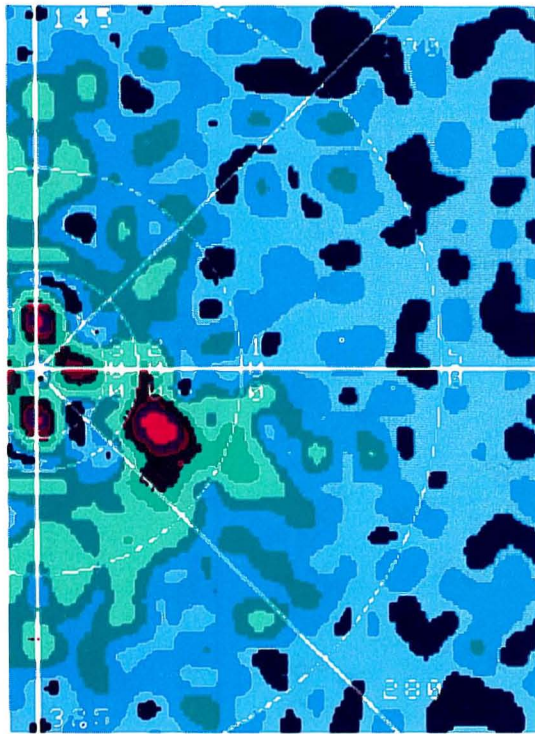
The various subscenes were examined as described earlier and the absolute power of the radar return calculated for the major peaks in the Fourier transforms. The calculation of this power required that corrections be made based on the results of the incidence angle dependences derived earlier. The results in the column marked "Average" in Table 3 have been used in this scaling. As well, it was necessary to correct the spectra derived from the scene which showed effects of antenna wobble. Information on peak orientations, power and wavelength were compiled from the individual spectra; that is averaging was not done. Originally, this was done because there appeared to be a number of common peaks identifiable in the overlapping subscenes. In the end, it proved that only 2 wave trains were consistently present, and therefore the results from these form the basis of the conclusions drawn later. These two wave trains were represented by the strongest returns in all of the spectra.

Figure 5 shows a sample of the spectra found from three overlapping subscenes. The wave orientation has been noted in degrees from range travelling. There is an obvious reduction in detection of the major peak as the wave train varies from range to azimuth travelling. A visual presentation of this dependence is shown in Figure 6. The crosses and boxes indicate individual data points derived from the two major peaks in the various Fourier transforms. These have been averaged in 10 degree bands and this average is represented in the histogram drawn as a solid line. No distinction has been made between waves oriented at the same angle but on different sides of range travelling. An initial impression is that the results are quite noisy. An examination shows that despite this there does appear to be a discernable trend to larger power returned for waves travelling in the range direction. The change in power from range to azimuth travelling waves is about 24 to 1.

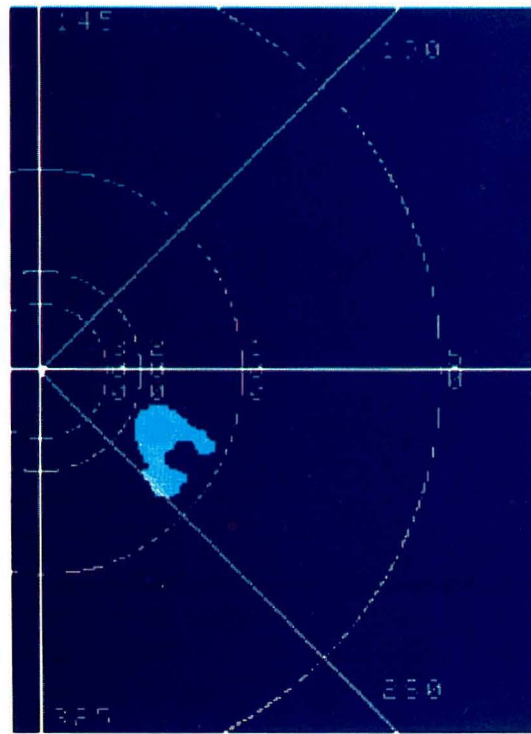
In each of the 10 degree bands from 0 to 30 degrees there are extreme values which were included in the histogram. If the largest extreme in each of these bands is discarded, the results are shown as the dashed histogram. The effects are quite evident. While the trend to lower power at larger aspect angles is preserved, the change in the power returned from range to azimuth travelling waves is about 16 to 1.

It was also decided to examine the dependence of the detected wavelength of the peak on the aspect angle. While others (Shuchman et al. 1983) had found no dependence, these data permitted another check of this. Figure 7 shows a plot of this. Again, crosses and boxes mark data points and the solid lines are averages in 10 degree bands. No dependence of the detected wavelength on the aspect angle is seen.

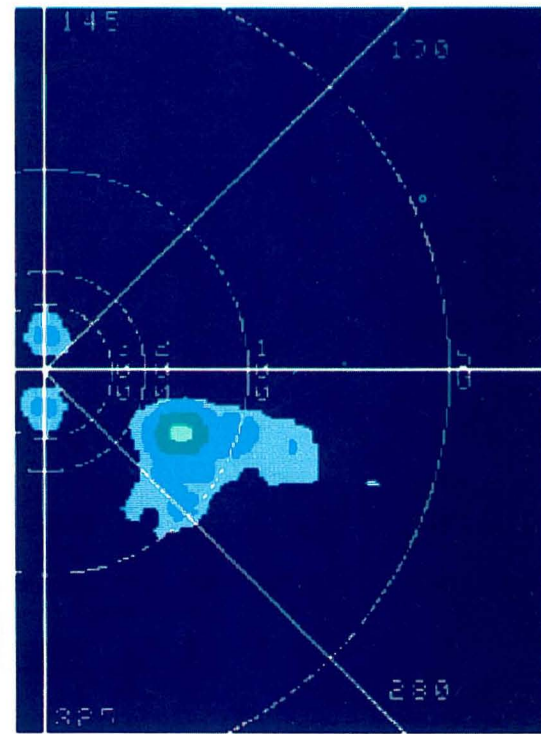
11



NEAR RANGE



MID RANGE



FAR RANGE

Figure 5. Look angle dependence for the major peak from overlapping subscenes.

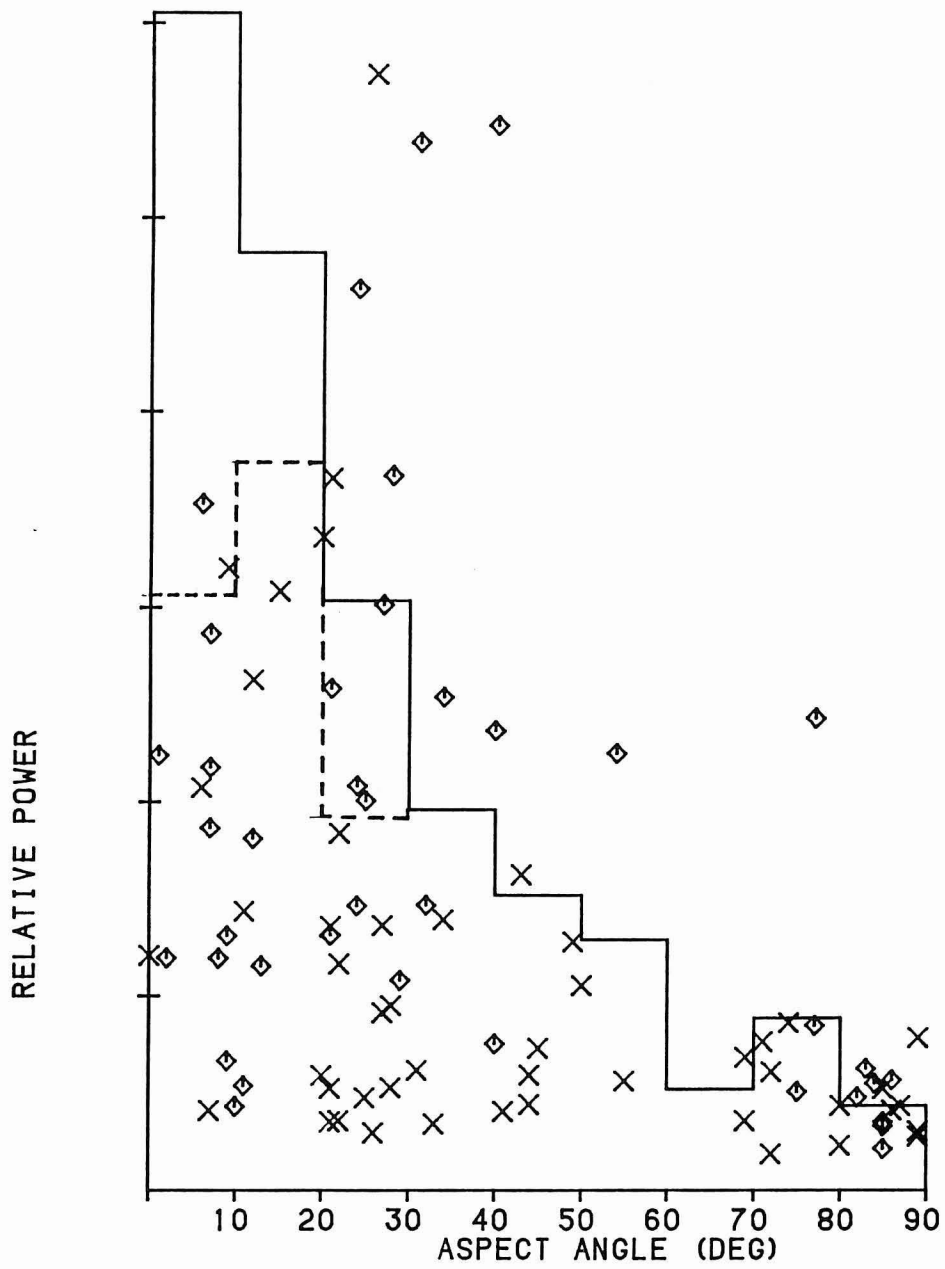


Figure 6. Look angle dependence of the strength of detected spectral peaks.

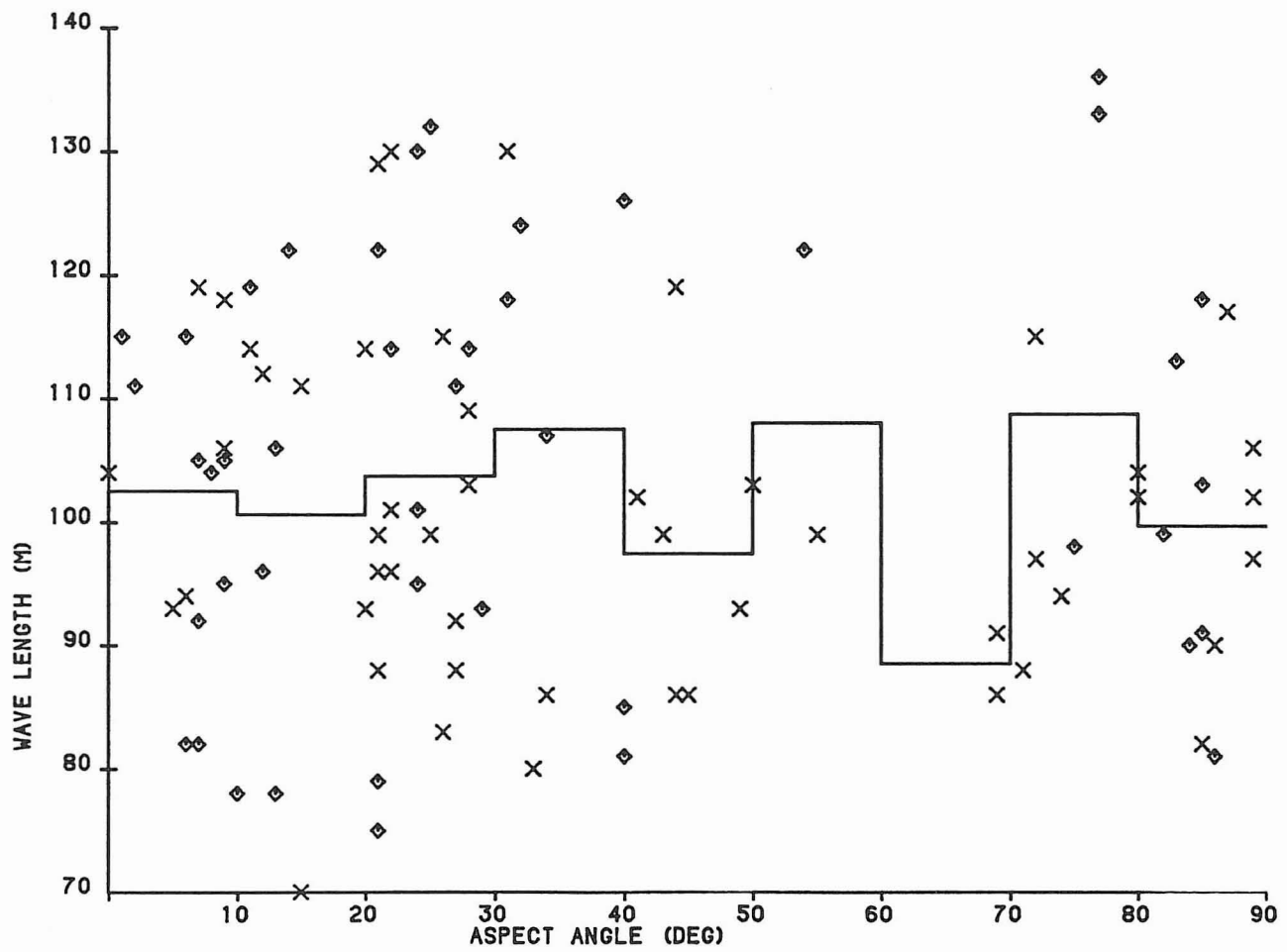


Figure 7. Wavelength of detected spectral peaks versus aspect angle.

Wind Speed and Wave Height Dependence

It is desirable to compile data on the sensitivity of a SAR to surface gravity waves under varying conditions of winds and waves. In the experiment described here, both wave heights and wind speeds were reduced from the first day to the second. However, quantitative comparisons of the power returned are difficult because the SAR was not calibrated. One way to treat this problem is to examine the signal to noise ratios from the different days. This can be done by calculating the mean strengths of the power returned from the dominant wave component each day to the background noise in the Fourier transform. The power of the components have been corrected for the radar incidence angle as described earlier. A simple functional fit has been made to the results presented in Figure 6, as well, so that this dependence can be removed. The mean signal to noise ratio is about 50% higher on March 15 compared to March 17. There was a substantial variation on each day. Nevertheless, these results support the qualitative impression that waves were imaged more clearly on March 15.

Conclusion

A number of factors were found that influenced the quality of the SAR data and hence affected the reliability of extracting wave information from SAR imagery. The first factor was due to uncorrected antenna motion. There was roughly a 5:1 variation in computed peak wave energies due to this factor. The incidence angle of the radar to the wave field was also examined. The results showed that there was a dramatic falloff in returned power as incidence angle increased. At high incidence angles, contamination from side lobes of the radar tended to increase the received power. There was also found to be a substantial falloff in relative power depending on the look angle of the radar to the propagation direction of the waves. Range travelling waves were the most readily detected. Over a 50 degree variation, there was a falloff to one fifth of the power received for range travelling waves. There were, however, no apparent effects on the detected wavelengths of the waves due to this factor. All of these results are predicted from radar theory. However, theory cannot yet take into account all of the complexities of an actual measured wave field. For this reason, the experiment was a useful exercise to gather real data to gauge the magnitude of these effects.

Acknowledgements

The author would like to thank the staff of the RADARSAT office for their help in making available their image analysis system in the processing of the SAR data. In particular, Dave Williamson is to be thanked for his diligent and careful work. Thanks are also due the staff at CCRS for flying the experiment and the initial data processing. Mobil Oil of Canada was most helpful in ensuring the observations from both meteorological and wave sensors were made properly, and for providing me with the processed wind data. Finally, I wish to thank Ron Wilson for permitting me to spend time on this project.

References

- Alpers, W.R., D.B. Ross and C.L. Rufenach. 1981. On the Detectability of Ocean Surface Waves By Real and Synthetic Aperture Radar. *J. Geophys. Res.* V86(C7): 6481-6498.
- Beal, R.C., P.S. DeLeonibus and I. Katz (ed). 1981. Spaceborne Synthetic Aperture Radar for Oceanography. John's Hopkins University Press, Baltimore.
- Brown, O.B. and R.E. Cheney. 1983. Advances in Satellite Oceanography. *In* U.S. National Report to International Union of Geodesy and Geophysics 1979-1982. Amer. Geophys. Union: 1216-1230.
- Fu, L. and B. Holt. 1982. SEASAT Views Oceans and Sea Ice with Synthetic Aperture Radar. Jet Propulsion Laboratory Publication 81-120, NASA: 200 p.
- Gonzales, F.I., R.C. Beal, W.E. Brown, J.F.R. Gower, D. Lichy, D.B. Ross, C.L. Rufenach and R.A. Shuchman. 1979. SEASAT Synthetic Aperture Radar: Ocean Wave Detection Capabilities. *Science* V204: 1418-1421.
- Keeley, J.R.. 1982. Comparison of Wave Measurements from a Synthetic Array Radar. Can. Tech. Rep. of Hydrogr. and Ocean Sci. No.6. Marine Environ. Data Serv., Dept. of Fisheries and Oceans: 31 p.
- Lapp, P.A. and D.J. Lapp. 1981. Preliminary Statement of User Requirements for Ice and Ocean Information. RADARSAT: Report 81-3.
- Raney, R.K. 1981. Wave Orbital Velocity, Fade, and SAR response to Azimuth Waves. *J. Oceanogr. Eng.*, October.
- Shuchman, R.A., W. Rosenthal, J.D. Lyden, D.R. Lyzenga, E.S. Kasischke, H. Gunther and H. Linne. 1983. Analysis of MARSEN X Band SAR Ocean Wave Data. *J. Geophys. Res.* V88(C14): 9757-9768.
- Vesecky, J.F., H.M. Assal and R.H. Stewart. 1981. Remote Sensing of the Ocean Waveheight Spectrum using Synthetic-Aperture-Radar Images. *In* Oceanography from Space, J.F.R. Gower (ed), Plenum Press, New York: 449-457.

